Princeton Plasma Physics Laboratory

PPPL- 4912

PPPL- 4912

Fast Wave Heating in the NSTX-Upgrade Device

Nicola Bertelli, et. al.

June, 2013

PPPL PRINCETON PLASMA PHYSICS LABORATORY

Prepared for the U.S. Department of Energy under Contract DE-AC02-09CH11466.

Princeton Plasma Physics Laboratory
Report Disclaimers

Full Legal Disclaimer

Trademark Disclaimer

PPPL Report Availability

Princeton Plasma Physics Laboratory:

http://www.pppl.gov/techreports.cfm

Office of Scientific and Technical Information (OSTI):

http://www.osti.gov/bridge

Related Links:

U.S. Department of Energy

Office of Scientific and Technical Information

Fusion Links

Fast wave heating in the NSTX-Upgrade device

N. Bertelli[*], E. F. Jaeger[†], L. Berry[**], P. T. Bonoli[‡], R. Budny[*], G.-Y. Fu[*], S. Gerhardt[*], D. L. Green[**], R. W. Harvey[§], J. C. Hosea[*], G. J. Kramer[*], B. LeBlanc[*], R. J. Perkins[*], C. K. Phillips[*], P. Ryan[**], G. Taylor[*], E. J. Valeo[*], J. R. Wilson[*] and J. C. Wright[‡]

[*]*Princeton Plasma Physics Laboratory, Princeton, NJ 08543 USA*
[†]*XCEL Engineering Inc., Oak Ridge, TN 37830, USA*
[**]*Oak Ridge National Laboratory, Oak Ridge, TN 37831-6169, USA*
[‡]*MIT Plasma Science and Fusion Center, Cambridge, MA 02139, USA*
[§]*CompX, Del Mar, CA 92014, USA*

Abstract. NSTX-Upgrade will operate with toroidal magnetic fields ($B_{\rm T}$) up to 1 T, nearly twice the value used in the experiments on NSTX, and the available NBI power will be doubled. The doubling of $B_{\rm T}$ while retaining the 30 MHz RF source frequency has moved the heating regime from the high harmonic fast wave (HHFW) regime used in NSTX to the mid harmonic fast wave (MHFW) regime. By making use of the full wave code AORSA, this work shows that direct ion damping (mainly by thermal ions localized at the 5th harmonic resonance) might be significant in NSTX-Upgrade under TRANSP predicted full performance conditions and the electron and ion absorption is sensitive to the ratio of electron and ion temperature. Launching at high toroidal wave number appears to be one way to significantly reduce the ion damping. By using the extended AORSA code, which includes a detailed description of the scrape-off layer in the field solutions, we found a large electric field amplitude outside of the last closed flux surface as previously seen in NSTX from AORSA simulations (D. L. Green, *et al*, *Phys. Rev. Lett.* **107**, 145001 (2011)). Preliminary results by introducing a collision damping in the scrape-off layer in the AORSA code to represent a damping process are presented, showing for the first time absorbed power in the scrape-off layer.

INTRODUCTION

Fast waves at high harmonics of ion cyclotron frequency have been used successfully on National Spherical Torus Experiment (NSTX) [1].They provide a promising heating and current drive option for the Fusion Nuclear Science Facility (FNSF) designs based on spherical torus (ST) [2], in which the plasma needs to be initiated, ramped-up and sustained fully non-inductively. NSTX-Upgrade, which is presently scheduled to be completed in 2014 [3], will operate with toroidal magnetic fields ($B_{\rm T}$) up to 1 T, nearly twice the value used in the experiments on NSTX, and the available NBI power will be doubled. The doubling of $B_{\rm T}$ while retaining the 30 MHz RF source frequency moves the heating regime from the high harmonic fast wave (HHFW) regime used in NSTX to the mid harmonic fast wave (MHFW) regime. In particular, for Deuterium majority ion and $B_{\rm T}(0) = 0.55$ T (as in NSTX) the harmonic resonances inside of the last closed flux surface range from the 2nd/3rd to the 11th whereas, for $B_{\rm T}(0) = 1$ T, the harmonic resonances inside of the last closed flux surface range from the 2nd to the 5th. In this work, power partitioning among the electron and various ion species during MHFW heating in an H-mode scenario planned for NSTX-Upgrade [4] is analyzed using the recent extended version of the full wave code AORSA [5], which takes into account the scrape-off layer [6] . We show electron thermal ion, and beam ion absorption as a function of antenna phase and the evaluation of the electric field inside and outside of the last closed flux surface. In addition, preliminary results of the power density inside and outside of the last closed flux surface by including a collision damping to represent a damping process in the scrape-off layer are also presented.

FULL WAVE MODELING RESULTS

In this paper we analyze an H-mode scenario being considered for NSTX-Upgrade obtained by using the free-boundary TRANSP code [4]. The magnetic field is $B(R_0) = 1$ T, and the plasma current is $I_{\rm p} = 1.1$ MA. Temperature and density

profiles of electrons and main ion (Deuterium) are shown in Figure 1(a) and 1(b), respectively. The central electron and ion temperatures are given by $T_e(0) = 1.22$ keV and $T_i(0) = 2.86$ keV, respectively. The central electron density is $n_e(0) = 1.1 \times 10^{20}$ m^{-3}, and the NBI power is $P_{NBI} = 6.3$ MW. In this analysis we assume the same temperature profile for thermal ion species (including impurities), while for the beam ions temperature (T_{bi}) we have adopted an effective temperature given by

$$T_{bi} = \frac{2}{3}\frac{E}{n_{fast}}, \tag{1}$$

where E and n_{fast} are the total energy density profile and the density of the beams ions, respectively. Both these quantities are provided by the TRANSP simulation. The beam ions concentration ($100 \times \frac{n_{fast}}{n_e}$) is about 2% in this specific case. In Figure 1(c), the electron density profile used in these numerical simulations is shown as a function of the major radius (R) in the edge of the plasma.

Figures 2 shows the absorption (in percentage) of electrons, thermal Deuterium (D), and beam ions (D_{beam}) as a function of the toroidal component of the wave vector, $k_\phi = n_\phi/R$ (where n_ϕ and R are the toroidal mode number and the major radius, respectively) obtained from AORSA. Three different cases have been performed which correspond to three different antenna phases: $|k_\phi| = 3, 8$, and 13 m^{-1} [7, 8]. Figure 2(a) shows the electron and ion absorption by using the electron and ion temperature profiles shown in Figure 1(b) (i.e., $T_i(0) = 2.86$ keV and $T_e(0) = 1.22$ keV), while in Figure 2(b) the ion temperature is lowered by 50% and the electron temperature is unchanged (i.e., $T_i(0) = 1.42$ keV and $T_e(0) = 1.22$ keV). In Figure 2(c), the ion temperature is again decreased by 50% but the electron temperature is doubled (i.e., $T_i(0) = 1.43$ keV and $T_e(0) = 2.44$ keV). In Figure 2(a), when $|k_\phi|$ increases, the electron absorption increases while the ion absorption decreases, in agreement with previous works on HHFW (see, for instance, [9, 10]). More specifically, relatively stronger absorption by thermal deuterium and beam ions is found predominantly at lower $|k_\phi|$. One possible explanation of such strong ion absorption is that the lower electron beta (beta is the ratio of plasma pressure to total magnetic field pressure) due to the higher magnetic field in NSTX-Upgrade might result in less direct electron absorption. Another possible reason is that the high value of the ion temperature with respect to the electron temperature (Figure 1(b)) can lead to higher ion absorption. From Figures 2(b) and 2(c) it can see that the electron absorption increases significantly when the T_i/T_e ratio is decreased, in particular, for $|k_\phi| \geq 8$ m^{-1}. This behavior is more evident in Figure 2(c) where T_e is much larger that T_i. At the same time, again more clearly in Figure 2(c), one sees a strong reduction of thermal D and beam ion absorption (for $|k_\phi| \geq 8$ m^{-1}). The antenna phase corresponding to $|k_\phi| = 3$ m^{-1} seems to be the more unfavorable for heating electrons, compared to $|k_\phi| = 8$ and 13 m^{-1}, for all three ratios of T_i/T_e analyzed.

Figures 3(a), and 3(b) show the contour plot of the electrons (3(a)) and thermal deuterium (3(b)) power density for $k_\phi = 8$ m^{-1} using density and temperature profiles shown in Figures 1(a) and 1(b), respectively. The electron absorption is spread across a wide region between the magnetic axis and the last closed flux surface. On the other hand, from Figure 3(b), one can see that the absorption of the thermal deuterium occurs in correspondence of the deuterium's harmonic resonances in the plasma. The 2nd to 5th harmonic resonances of deuterium are within the last closed flux surface and the deuterium power density is mainly absorbed at the 5th deuterium harmonic resonance, the closest to the magnetic axis. For a better visualization, see also Figure 4(a) which shows the 1D flux surface averaged power density of electrons, thermal deuterium, and beam ions as a function of the square root of the normalized poloidal flux.

Figure 3(c) (3(d)) shows the two dimensional AORSA results for the real part of the parallel electric field (in V/m) with (without) a scrape-off layer region, for $k_\phi = 8$ m^{-1}. The main differences in these two figures is the strong electric field amplitude found in the scrape-off layer when the scrape-off layer is taken into account with respect to the case without scrape-off layer. One can also note that, inside of the last closed flux surface, no big differences appear in the parallel electric field for both cases. So far, no specific damping in the scrape-off region has been included, therefore no absorbed power has been found outside of the last closed flux surface, in contradiction to experimental studies of HHFW heating on the NSTX, which have demonstrated that substantial HHFW power loss occurs along the open field lines in the scrape-off layer [11]. For this reason we inserted a collisional loss in the scrape-off layer of AORSA to serve as a proxy for the damping processes there. Note that the scrape-off layer can be considered to be like a cavity with open field lines striking the divertor plates top and bottom, and bounded radially by the last closed flux surface and the wall structures. Preliminary results of the flux surface averaged power density profiles are shown in Figure 4 including a collision damping for $\rho \geq 0.8$, for the NSTX-U case discussed above. In Figure 4(a) no collision damping is considered while in Figures 4(b) , 4(c) and 4(d), an effective collisional term equal to $\nu/\omega = 0.01$, 0.05, and 0.1 is used, respectively (ν is the effective electron-ion collision frequency). Power density outside of the last closed flux surface increases when ν/ω increases. This behavior is more significant for the thermal Deuterium. Furthermore,

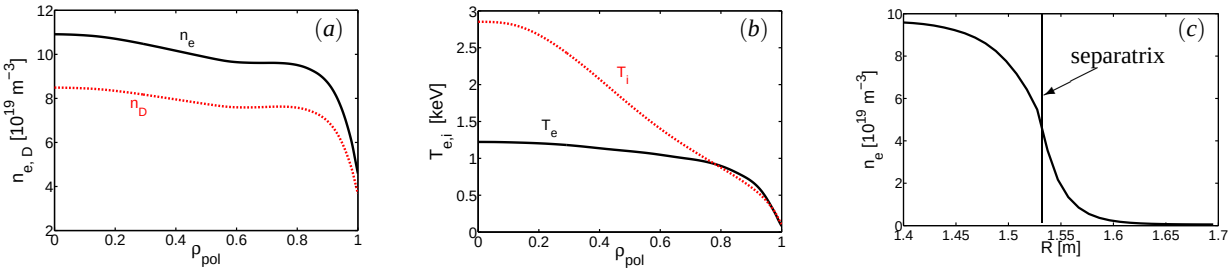

FIGURE 1. Density (Figure (a)) and temperature (Figure (b)) profiles of electron (solid line) and the thermal Deuterium (dashed line) as a function of the square root of the normalized poloidal flux, $\rho_{\rm pol}$. Figure (c) shows the electron density profile in the edge of the plasma as a function of the major radius (R).

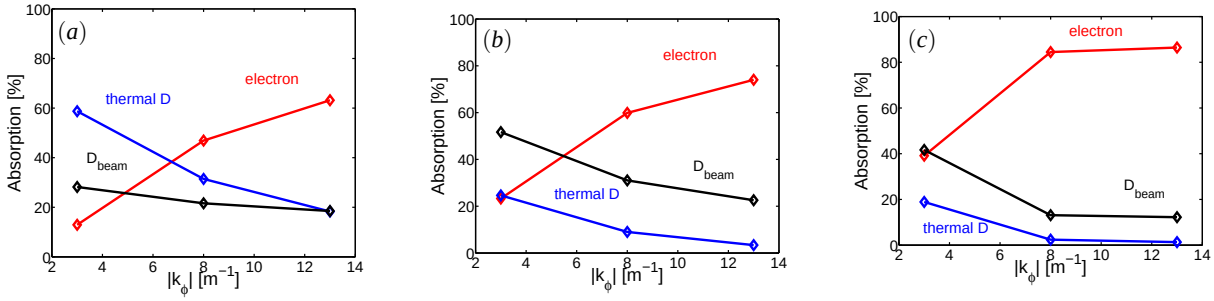

FIGURE 2. Absoprtion of electrons, thermal Deuterium (D), and fast ions ($D_{\rm beam}$) as a function of the toroidal component of the wave vector (k_ϕ) for a H-mode scenario considered for NSTX-Upgrade [4] obtained from AORSA simulations including the scrape-off layer. Figure (a): using electron and ion temperatures shown in Figure 1(b); Figure (b): decreasing $T_{\rm i}$ by 50% ($T_{\rm i}(0) = 1.43$ keV) but $T_{\rm e}$ the same as in Figure 1(b) ($T_{\rm e}(0) = 1.22$ keV); Figure(c): decreasing $T_{\rm i}$ by 50% ($T_{\rm i}(0) = 1.43$ keV) and doubling $T_{\rm e}$ relative to that used in (a) and (b) ($T_{\rm e}(0) = 2.44$ keV).

absorbed power outside of the last closed flux surface is found roughly of the same order of that evaluated in some NSTX discharges [12] when about $\nu/\omega \geq 0.05$ which is considerably larger than the $\nu/\omega \sim 0.005$ obtained with Spitzer resistivity. Further and more detailed simulations on this last point are being investigated for both NSTX and NSTX-U and the magnitude of the edge collisional losses will then be used to evaluate possible potential damping mechanisms in the scrape-off layer in order to identify which physical mechanism (or combination of mechanisms) causes HHFW power loss along the open field lines in the scrape-off layer.

CONCLUSIONS

Full wave numerical analysis for an H-mode scenario planned in NSTX-Upgrade has been shown. The dependency of the electron and ion absorption with respect to the antenna phase has been presented. We found that electron (ion) absorption increases (decreases) when wave toroidal number increases. Launching at low wave number ($|k_\phi| = 3$ m^{-1}) appears to be unfavorable for electron heating, and, by inference, direct RF current drive due to the higher ion absorption. Power partitioning between the electron and the ions is strongly dependent on the ratio of $T_{\rm i}/T_{\rm e}$, and the condition $T_{\rm e} > T_{\rm i}$ results in a significantly higher electron heating, in particular, for $|k_\phi| \geq 8$ m^{-1}. It has also been shown that electron power absorption is spread out between the magnetic axis and the last closed flux surface while the thermal deuterium power density is localized at the harmonic resonances and predominantly at the 5th deuterium resonance harmonic. Finally, a large electric field amplitude outside of the last closed flux surface has been found which might be associated with the scrape-off layer power losses observed in NSTX. Preliminary results of the power density, for this specific NSTX-U case, by inserting collisional losses in the scrape-off layer of AORSA, show significant absorbed power outside of the last closed flux surface for $\nu/\omega \geq 0.05$ which is considerably larger than the

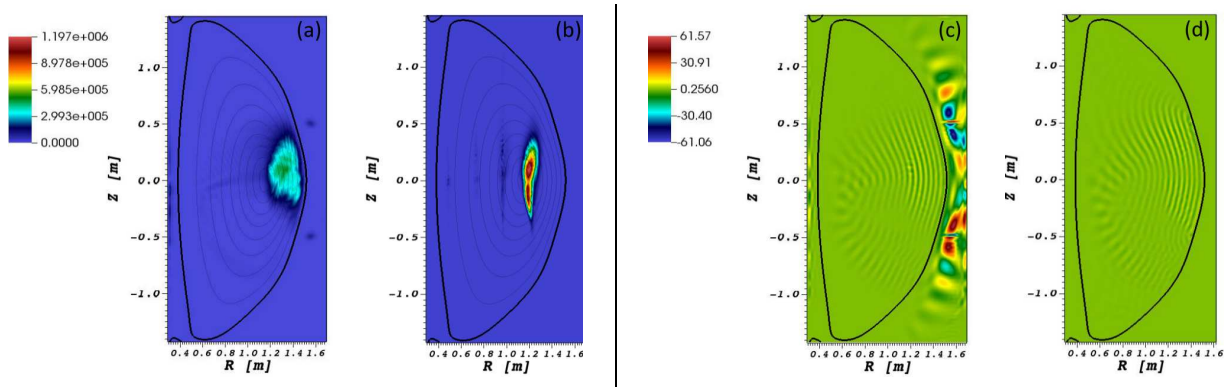

FIGURE 3. Figures (a) and (b): contour plots of the power density (in W/m^3) absorbed by electron (a) and thermal Deuterium (b) for the NSTX-U case with $k_\phi = 8$ m^{-1}. Both figures are plotted with the same color scale. Figures (c) and (d): two dimensional AORSA results of the real part of the parallel electric field (in V/m) with scrape-off layer (a) and without scrape-off layer (b) for the NSTX-U case with $k_\phi = 8$ m^{-1}. Figures (a) and (b) ((c) and (d)) are plotted with the same color scale.

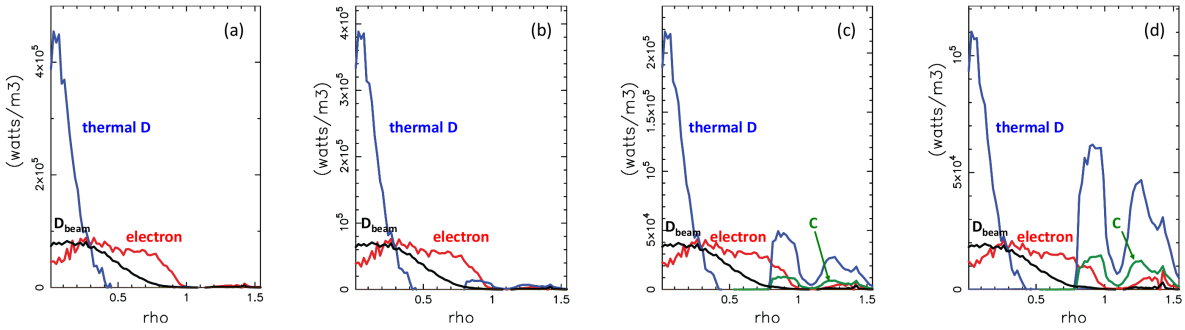

FIGURE 4. Flux surface averaged power density of electrons, thermal Deuterium, and beam ions as a function of the square root of the normalized poloidal flux, for NSTX-U case with $k_\phi = 8$ m^{-1}. (a): no collision damping, (b): collision damping with $\nu/\omega = 0.01$, (c): collision damping with $\nu/\omega = 0.05$, and (d): collision damping with $\nu/\omega = 0.1$. Note that different scales in y-axis are used.

$\nu/\omega \sim 0.005$ obtained with Spitzer resistivity, suggesting the damping scale of the loss mechanism. Further and more detailed simulations on this last point are being investigated for both NSTX and NSTX-U.

Acknowledgments. This work was supported by the SciDAC Center for Wave-Plasma Interactions Contract No. DE-FC02-01ER54648 and US Department of Energy (DOE) Contract DE-AC02-CH0911466.

REFERENCES

1. M. Ono *et al*, *Nucl. Fusion* **40**, 557 (2000).
2. Y.-K. Peng *et al*, *Plasma Phys. Control. Fusion* **47**, B263 (2005).
3. J. E. Menard *et al*, *Nucl. Fusion* **52**, 083015 (2012).
4. S. P. Gerhardt, R. Andre, and J.E. Menard *Nucl. Fusion* **52**, 083020 (2012).
5. E. F. Jaeger *et al*, *Phys. Plasmas* **8**, 1573 (2001).
6. D. L. Green *et al*, *Phys. Rev. Lett.* **107**, 145001 (2011).
7. J. Hosea *et al*, *Phys. Plasmas* **15**, 056104 (2008).
8. G. Taylor *et al*, *Phys. Plasmas* **17**, 056114 (2010).
9. C. N. Lashmore-Davies, V. Fuchs, and R. A. Cairns, *Phys. Plasmas* **5**, 2284 (1998).
10. J. Menard *et al*, *Phys. Plasmas* **6**, 2002 (1999).
11. R. J. Perkins *et al*, *Phys. Rev. Lett.* **109**, 045001 (2012).
12. R. J. Perkins *et al*, Invited Paper at this Conference.

The Princeton Plasma Physics Laboratory is operated
by Princeton University under contract
with the U.S. Department of Energy.

Information Services
Princeton Plasma Physics Laboratory
P.O. Box 451
Princeton, NJ 08543

Phone: 609-243-2245
Fax: 609-243-2751
e-mail: pppl_info@pppl.gov
Internet Address: http://www.pppl.gov